Mahadevamurty Nemani[1]
Graduate Student.

Tsu-Chin Tsao
Assistant Professor.

Department of Mechanical and Industrial Engineering.

Seth Hutchinson
Assistant Professor.

Department of Electrical and Computer Engineering.

University of Illinois at Urbana-Champaign, Urbana, IL 61801

Multi-Rate Analysis and Design of Visual Feedback Digital Servo-Control System

This paper addresses the analysis and design of digital motion control system with machine vision as a feedback measurement in the servo loop. The camera vision is modeled as a discrete time-delayed sensor. A multirate formulation is proposed based on the fact that vision update rate is slower than the digital servo-control update rate and is analyzed through the lifting technique which converts the periodic time varying multirate system to a time invariant one. Some interesting properties of this specific multirate system are found and are utilized in control system design. An l-1 norm optimal control problem is formulated to minimize the maximum time domain error, which has direct connection to camera field of view and mechanical tolerance. A numerical example is given to demonstrate the presented methods.

1 Introduction

The integration of computer vision with robot motion control has steadily progressed, from early look and move systems in which vision was used to recognize and locate an object prior to its manipulation, to current systems in which visual feedback is incorporated into an outer control loop, closing the position feedback loop around the end effector (rather than around the joint encoders) (Allen et al., 1991; Feddema et al., 1989; Papanikolopoulas et al., 1991; Skaar et al., 1987; Weiss et al., 1987). To date these systems use vision feedback to generate set points that are sent to the low level joint controllers. None of the methods reported have used visual feedback in the servo-level control. In order to enhance the speed and accuracy performance, it becomes necessary to address the dynamic interactions between the faster servo inner loop and the slower visual outer loop, and eventually to incorporate visual feedback in the servo-loop directly. This motivates us to look at the analysis and design of high performance visual feedback control systems, in which the dynamic characteristics of the visual sensing element cannot be neglected.

Typically, a visual feedback system has components evolving at two different rates, hence, giving rise to a multirate system. Multirate sampling theory has been studied well in connection with multirate digital filter design. Meyer et al. (1975) showed that multirate systems are special cases of periodic systems. In terms of multirate control problems, Rahmani et al. (1990) solved the LQR problem for continuous-time multirate sampling systems under the assumption that the control input is piecewise continuous, and obtained a periodic state feedback solution by solving a discrete algebraic riccati equation. They pointed out that even when the measurements are obtained at a slow rate relative to the control input rate, the multirate strategy leads to improvements in the performance index when compared with single rate sampling systems. However, their assumption that system state was available for measurement is generally not the case in vision measurement. Dahleh et al. (1992) solved for the optimal controllers for periodic and hence, multirate systems using the "lifting technique," which has been studied in detail by Khargonekar et al. (1985), Francis et al. (1988) and Bamieh et al. (1992), to convert a periodic system into a higher dimensional time invariant system. They proposed a method by which the causality constraints on the controller, which come from the lifting, can be converted into linear constraints. In this paper we will utilize the lifting technique for a special class of multirate problems—the visual feedback systems and gain specific insights not addressed previously.

Once the original time varying multirate problem has been reformulated as a time invariant problem by the lifting technique, any known linear design technique can be applied to the lifted problem. In this paper, we choose to solve an *l*-1 optimal control problem based on two reasons. First, the vision sensor unlike other sensors has a bounded field of view, i.e., the object must always (at all times) remain within the camera field of view. This implies that the maximum position error between the object and the camera must always lie within a certain limit. Second, the tolerance of mechanical motion systems, such as robots or machine tools, is specified in terms of the maximum error. Also, effects due to uncertainties in the measurement of the position of the object by the camera (due to limited resolution of vision systems) and errors due to image processing are naturally incorporated since a worst case design is performed. Minimizing the maximum tracking errors for the whole class of signals corresponding to the object motion

[1] Currently with Coordinated Science Laboratory, University of Illinois at Urbana-Champaign.

Contributed by the Dynamic Systems and Control Division for publication in the JOURNAL OF DYNAMIC SYSTEMS, MEASUREMENT, AND CONTROL. Manuscript received by the DSCD October 13, 1992, revised manuscript received March 18, 1993. Associate Technical Editor: J. L. Stein.

Copyright © 1994 by ASME
Downloaded 08 Sep 2010 to 130.126.137.86. Redistribution subject to ASME license or copyright; see http://www.asme.org/terms/Terms_Use.cfm

leads to the l-1 optimal control problems, which has been studied by Vidyasagar (1986), Dahleh et al. (1987), McDonald et al. (1991), Diaz-Bobillo (1992).

The contributions of this work are summarized as follows:

(a) We model the vision feedback control system as a multirate system, in which the vision element has been modeled as a sampled-data sensor with a gain and a delay and the controller is updated at a faster sampling rate than the vision element.

(b) We utilize the lifting technique for the analysis and design of the multirate control system and show that the control problem can be formulated as a two-block problem; that the causality constraints on the controller are automatically satisfied and need not be explicitly accounted for; and that any periodic controller in the lifted domain can have a time invariant realization.

(c) We demonstrate the design methodology, i.e., the lifting and l-1 optimal control, with a numerical example on an existing mechanical system and compare the performance with conventional PD controller at different sampling rates.

The rest of this paper is organized as follows: Section 2 briefly describes the lifting technique in brief; Section 3 models the vision sensor and formulate the multirate control problem; Section 4 formulates the l-1 optimization problem; Section 5 gives state space realization for the lifted system; Section 6 presents a numerical example and discusses the results followed by the conclusions in Section 7.

2 The Lifting Technique

We briefly discuss the Lifting technique presented in Francis et al. (1988). The following notations are adopted. g (lower case) is a signal and G (upper case) is a system in the continuous time domain, $\bar{g}$ and $\bar{G}$ are in the discrete time domain, and $\tilde{g}$ and $\tilde{G}$ are in the lifted domain. S_T refers to a sampler with sampling time T, and H_T refers to a zero-order hold with sampling time T.

Consider a complex space $\mathbf{S}(C^n)$ of C^n values sequences defined on the set [0, 1, 2, ...]. The direct sum of m copies of $\mathbf{S}$ is represented as $\mathbf{S}^m$. The subspace of square summable sequences on $\mathbf{S}$ is represented as h_2 and similarly on $\mathbf{S}^m$ by h_2^m.

Every linear transformation has a matrix representation with respect to basis vectors of $\mathbf{S}$. The right shift operator Λ shifts a discrete sequence $u(k)$. Such that

$$\bar{y}=\Lambda\bar{u}$$
$$\bar{y}(k+1)=\bar{u}(k) \quad k\geq 0$$
$$\bar{y}(0)=0.$$

Its adjoint Λ^* shifts a discrete sequence $u(k)$ s.t.

$$\bar{y}=\Lambda^*\bar{u}$$
$$\bar{y}(k-1)=\bar{u}(k) \quad k\geq 0$$

Notice that $\Lambda\Lambda^*=\Lambda^*\Lambda=\mathrm{I}$. A system $\bar{G}$ is said to be shift invariant iff

$$\Lambda^*\bar{G}\Lambda=\bar{G} \tag{2.1}$$

and is n periodic iff

$$\Lambda^{*n}\bar{G}\Lambda^n=\bar{G} \tag{2.2}$$

Notice the difference between n periodicity and shift invariance. A shift invariant system is n periodic for any n but a n periodic system satisfies (2.2) only for a particular n and its multiples.

Two adjoint linear transformations are defined:

$\bar{y}=\bar{S}_m\bar{u}\Longleftrightarrow\bar{y}(k)=\bar{u}(mk)$; where m is an integer.

$$\bar{y}=\bar{S}_m^*u\Longleftrightarrow\bar{y}(k)=\begin{cases}\bar{u}(k/m) & \text{if } m \text{ divides } k\\ 0 & \text{else}\end{cases}$$

Given a particular discrete sequence $\bar{u}(k)$, one interpretation of $\bar{S}_m$ and $\bar{S}_m^*$ could be that $\bar{S}_m$ is a slow sampling of $\bar{u}$, i.e., it picks up only those impulses which are multiples of m, whereas $\bar{S}_m^*$ could be considered to be a fast sampling of the sequence $\bar{u}(k)$, i.e., it inserts zeroes between samples. Some facts which are a natural consequence of the definitions are

$$\Lambda\bar{S}_m=\bar{S}_m\Lambda^m \tag{2.3}$$

$$\Lambda^*\bar{S}_m=\bar{S}_m\Lambda^{*m} \tag{2.4}$$

$$\bar{S}_m\bar{S}_m^*=I\,(\bar{S}_m^*\bar{S}_m\neq I) \tag{2.5}$$

This result shows the noncommutative property of the operators $\bar{S}_m$ and $\bar{S}_m^*$. Roughly speaking, this means that the original signal can be obtained by first sampling it fast and then sampling it slow but not vice versa. Also

$$\bar{S}_m\Lambda^i\bar{S}_m^*=0 \quad \text{for } i=1,\ 2,\ \ldots\ (m-1) \tag{2.6}$$

The lifting technique provides a method by which periodic systems can be converted into a higher dimensional time invariant system. Consider the linear transformation

W: $\mathbf{S}\rightarrow\mathbf{S}^m$

$$W:\ \{\bar{u}(0),\ \bar{u}(1),\ \ldots.\}\rightarrow\left[\begin{pmatrix}\bar{u}(0)\\ \bar{u}(1)\\ \vdots\\ \bar{u}(m-1)\end{pmatrix},\begin{pmatrix}\bar{u}(m)\\ \bar{u}(m+1)\\ \vdots\\ \bar{u}(2m-1)\end{pmatrix}\ldots\ldots\right] \tag{2.7}$$

The operator W groups the first m elements of the sequence into a single vector, the next m elements into another vector and so on, i.e.,

$$W:=\begin{bmatrix}\bar{S}_m\\ \bar{S}_m\Lambda^*\\ \vdots\\ \bar{S}_m\Lambda_{m-1}^*\end{bmatrix} \tag{2.8}$$

The first row of operator W picks up elements of $\{\bar{u}\}$ which are m time units apart. The second row picks up the elements of a signal, obtained by time shifting $\{\bar{u}\}$ to the left by one, which are m time units apart, and so on.

The adjoint operator W^*: $\mathbf{S}^m\rightarrow\mathbf{S}$, i.e.,

$$W^*:=\left[\begin{pmatrix}\bar{u}(0)\\ \bar{u}(1)\\ \vdots\\ \bar{u}(m-1)\end{pmatrix},\begin{pmatrix}\bar{u}(m)\\ \bar{u}(m+1)\\ \vdots\\ \bar{u}(2m-1)\end{pmatrix}\ldots..\right]$$
$$\rightarrow\{\bar{u}(0),\ \bar{u}(1),\ \bar{u}(2),\ \ldots\} \tag{2.9}$$

$$W^*:=[\bar{S}_m^*\Lambda\bar{S}_m^*\ldots\Lambda^{m-1}\bar{S}_m^*] \tag{2.10}$$

Hence, W^* does the opposite of W. Intuitively, we expect $WW^*=I$. This can be verified as follows.

$$WW^*:=\begin{bmatrix}\bar{S}_m\\ \bar{S}_m\Lambda^*\\ \vdots\\ \bar{S}_m\Lambda_{m-1}^*\end{bmatrix}[\bar{S}_m^*\Lambda\bar{S}_m^*\ldots\Lambda^{m-1}\bar{S}_m^*]$$

$$\bar{S}_m\bar{S}^*{}_m=\bar{S}_m\Lambda^*\Lambda\bar{S}_m^*=\ldots=\bar{S}_m\Lambda^{*m-1}\Lambda^{m-1}\bar{S}_m^*=I$$

Also, note that

$$\bar{S}_m\Lambda^*\bar{S}_m^*=0$$

Hence, we get

$$WW^*=I \tag{2.11}$$

Similarly,

$$W^*W=I. \tag{2.12}$$

Downloaded 08 Sep 2010 to 130.126.137.86. Redistribution subject to ASME license or copyright; see http://www.asme.org/terms/Terms_Use.cfm

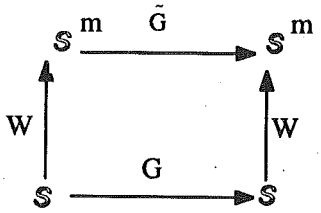

Fig. 2.1 Commutative diagram

This is a useful result and will be used extensively in Section 3. Noting that

$$W\Lambda^m = \Lambda W \tag{2.13}$$

In general, if $\overline{G}$ is m-periodic, i.e.,

$$\Lambda^m \overline{G} = \overline{G}\Lambda^m \tag{2.14}$$

it can be lifted to a shift invariant system of higher dimension. This can be seen in Fig. 1.

$$\tilde{G}: \mathbf{S}^m \rightarrow \mathbf{S}^m \text{ (the lifted plant)}$$

$$\tilde{G} = W\overline{G}W^* \tag{2.15}$$

These relationships are illustrated in Fig. 2.1.

It can be shown that $\tilde{G}$, which corresponds to the lifting of $\overline{G}$, is shift invariant. Therefore, known design techniques can be applied to $\tilde{G}$. Another important feature of lifting is that it is an isometry, i.e., the norm of the system is preserved by lifting. This can be verified as follows: We know from (2.15):

$$\tilde{G} = W\overline{G}W^*$$

It can be easily verified by definitions that $\|W\| = \|W^*\|$. Also, from (2.11) and (2.12) $WW^* = W^*W = I$, we have $\|W\| = \|W^*\| = 1$.

$$\Rightarrow \|\tilde{G}\| = \|W\overline{G}W^*\| \leq \|\overline{G}\| \tag{2.16}$$

Also, $\overline{G} = W^*\tilde{G}W$

$$\Rightarrow \|\overline{G}\| \leq \|\tilde{G}\| \tag{2.17}$$

Combining (2.16) and (2.17) we get

$$\|\overline{G}\| = \|\tilde{G}\| \tag{2.18}$$

3 Vision System Modeling and Multirate Problem Formulation

The block diagram of the plant with the camera in the feedback loop is shown in Fig. 3.1. The plant of concern here is assumed to be linear time invariant. The camera normally used in vision systems is a CCD camera. It has an inherent property of generating a discrete output. It is generally not associated with any dynamics and it essentially converts visual information into electrical signals. Associated with the camera is the vision unit which computes the relative position and the orientation of the object with respect to the camera by processing the image. Henceforth, the camera with the vision unit will be referred to as the camera. If the mapping from the object space to the image plane were unique and independent of the orientation of the object, the transformation from the input to the output of the camera would be the identity matrix, i.e., the gain of the camera unit is I (identity). However, this is typically not the case as the mapping is position dependent and is non unique with respect to the depth of the object. Also, there is a significant delay associated with the image processing unit, as image processing is computationally intensive. Here, we assume that the depth of the object with respect to the camera remains unchanged. This allows us to assume that the camera gain is I. Hence, the camera in our case has been modeled as a gain multiplied by a delay. In Fig. 3.1 the sampler, S_T, which precedes the camera is introduced to account for the inherent discrete nature of the camera. The controller is assumed to be discrete with a sampling rate T/m, where T is the sampling rate of the vision system (which is also the delay associated with the camera).

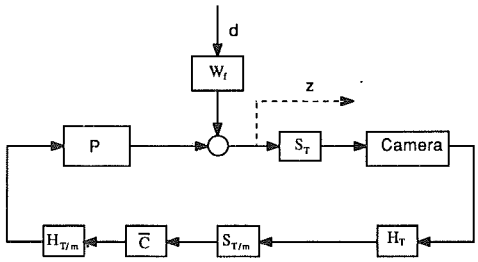

Fig. 3.1 Block diagram of the vision system

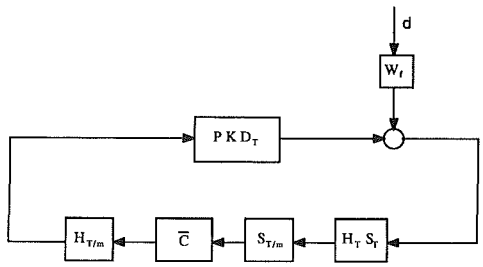

Fig. 3.2 Block diagram after substitution of camera model

The problem setup involves sampler and hold functions operating at two different sampling rates, i.e., the problem is multirate by nature. As it is intended to make the robot grasp a moving object the design objective is to minimize the tracking error, which is the relative error between the object and the robot end effector, given by z. The motion of the object is assumed to be unknown. Hence, the design problem turns out to be a worst case design as it is intended to keep the error to as small a value as possible irrespective of the motion of the object.

In Fig. 3.1 it is shown that the exogenous input, d, enters the system through a filter. But, in reality this is not the case. The reasons for introducing the filter are the following: (a) A strictly causal filter would make the design problem feasible as will be noted later. (b) The filter allows us to weight the signals in the desired frequency range, which here would be the low frequency range.

The problem deals with signals of both continuous and discrete nature. Strictly speaking one should minimize the error in continuous time. But here we minimize z in discrete time. This means that the controller which is optimal in the discrete domain is only suboptimal in the continuous sense. But, we can make the difference (in the performance) as small as possible. This is achieved by sampling the error as closely as possible. This, in our problem, manifests itself as generating discrete control signals as fast as possible.

Figure 3.1 can be redrawn as shown in Fig. 3.2. Notice that the delay operator (which corresponds to the delay of the camera) commutes with sample and hold operators as long as it is an integral multiple of the sampling times of the sample and hold operators. This is because the sample and hold operators are periodic with respect to T/m. From now on P will refer to PD_T, where D_T refers to a delay of T seconds. Note that D_T comes from the camera and due to its commutative property can be absorbed into the plant.

Rearranging the elements in Fig. 3.2 and converting the problem into a standard form we obtain Fig. 3.3. One must note H_TS_T is bounded only if it is preceded by a strictly causal filter. This implies that the filter we choose has to be strictly causal. The plant model we use is strictly causal. Hence the choice of a strictly causal filter guarantees the boundedness of H_TS_T.

Now, we will rewrite the elements as in Fig. 3.4, the reasons for which will be obvious as we proceed. The operator

Downloaded 08 Sep 2010 to 130.126.137.86. Redistribution subject to ASME license or copyright; see http://www.asme.org/terms/Terms_Use.cfm

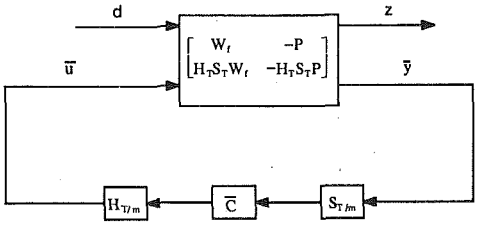

Fig. 3.3 Representation in the standard problem form

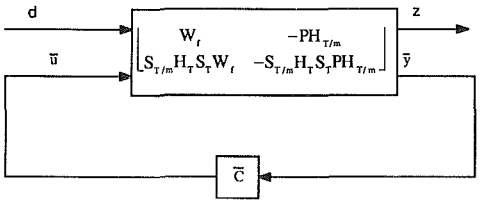

Fig. 3.4 Equivalent block diagram of Fig. 3.3

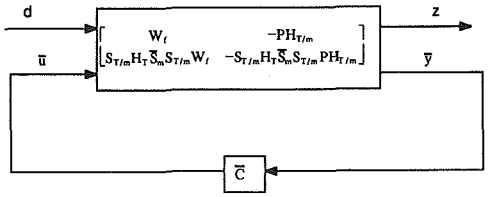

Fig. 3.5 Equivalent block diagram of Fig. 3.4

$S_T PH_{T/m}$ maps discrete time signals to discrete time signals. But, the operator is not shift invariant. The operator $S_T PH_{T/m}$ can be rewritten as

$$S_T PH_{T/m} = \bar{S}_m S_{T/m} PH_{T/m} \tag{3.1}$$

This follows from the fact that S_T, which is a slow sampler, samples the continuous time output of the plant every T seconds and generates a discrete output. This is equivalent to sampling the continuous time output of the plant at T/m sampling rate and picking only those samples which are m steps apart. This is the function of the operator $\bar{S}_m$ defined in the previous section. Similarly, $S_T W_f$ can be rewritten as

$$S_T W_f = \bar{S}_m S_{T/m} W_f \tag{3.2}$$

Therefore, incorporating the aforementioned changes into Fig. 3.4 yields Fig. 3.5. Using the transformations W and W^* defined previously and noting that $WW^* = W^*W = I$ from (2.11) and (2.12), rewrite the elements in Fig. 3.5 as

$$\begin{aligned} S_{T/m}H_T\bar{S}_m S_{T/m} W_f &= W^* W S_{T/m}H_T\bar{S}_m W^* W S_{T/m} W_f \\ &= W^* (W S_{T/m}H_T\bar{S}_m W^*)(W S_{T/m} W_f) \end{aligned} \tag{3.3}$$

Similarly,

$$\begin{aligned} &S_{T/m}H_T\bar{S}_m (S_{T/m} PH_{T/m}) \\ &\quad = W^* W S_{T/m}H_T\bar{S}_m W^* W (S_{T/m} PH_{T/m}) W^* W \\ &\quad = W^* (W S_{T/m}H_T\bar{S}_m W^*)(W S_{T/m} PH_{T/m} W^*) W \end{aligned} \tag{3.4}$$

and

$$PH_{T/m} = PH_{T/m} W^* W = (PH_{T/m} W^*) W \tag{3.5}$$

Define

$$H := W S_{T/m}H_T\bar{S}_m W^* \tag{3.6}$$

Introducing these modified operators into their respective places, we get Fig. 3.6. One must note that the application of

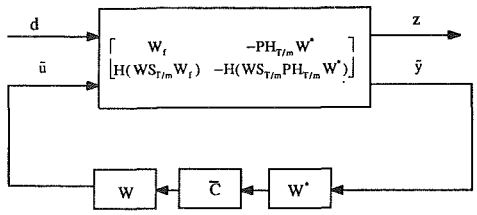

Fig. 3.6 Equivalent block diagram of Fig. 3.5

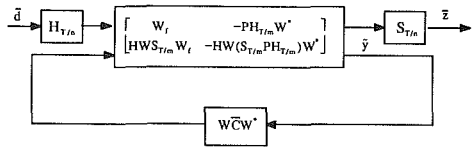

Fig. 3.7 Discrete approximation of Fig. 3.6

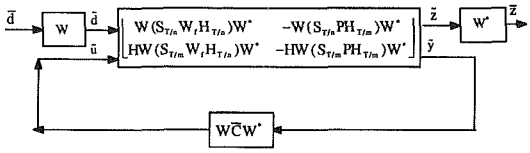

Fig. 3.8 Block diagram in lifted domain for Fig. 3.7

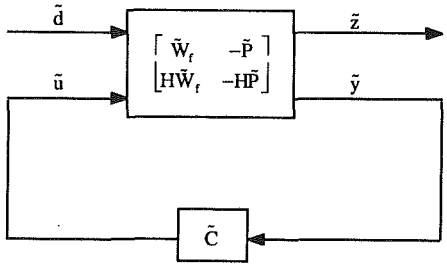

Fig. 3.9 Block diagram for the lifted system when $n = m$

transformations has changed the measurement output from a scalar to a vector signal

$$\tilde{y} = W\bar{y} \tag{3.7}$$

i.e., the measurement signal has been lifted.

Similarly

$$\tilde{u} = W\bar{u} \tag{3.8}$$

The controller $W\bar{C}W^*$ is the lifted version of the controller $\bar{C}$. Also, $W(S_{T/m}PH_{T/m})W^*$ is the lifted version of the discrete plant $S_{T/m}PH_{T/m}$.

It is important to note at this point that the problem represented by Fig. 3.6 is the same as that represented by Fig. 3.1. However, this problem involves mixed signals and one approach to solve it would be to perform a continuous time lifting on Fig. 3.6 (Bamieh et al., 1992). Another approach would be to solve an approximate discrete problem by introducing a fictitious sample and hold with sampling rate T/n at signals z and d, respectively. This discrete problem, as n tends to infinity, converges to the original problem in Fig. 3.1 (Dullerud et al., 1992). In this paper we adopt the second approach. With this modification Fig. 3.6 is redrawn as Fig. 3.7. By introducing the transformations W and W^* we get

$$\tilde{d}(k) = W\bar{d}(k), \tag{3.9}$$

$$\tilde{z}(k) = W\bar{z}(k), \tag{3.10}$$

Downloaded 08 Sep 2010 to 130.126.137.86. Redistribution subject to ASME license or copyright; see http://www.asme.org/terms/Terms_Use.cfm

where $\tilde{d}$ and $\tilde{z}$ are the lifted vector signals. The lifted system becomes as shown in Fig. 3.8.

To summarize, Fig. 3.8 is equivalent to Fig. 3.1 as n tends to infinity. The solution for the problem represented by Fig. 3.8 can be obtained using the approach of Meyer (1990). For the case when n is an integer multiple of m, the system in Fig. 3.8 can be lifted to a I/O space corresponding to T/n. To simplify the presentation we perform the design for the case $n=m$. In that case, we obtain Fig. 3.9.

Let,

$$(S_{T/m}W_fH_{T/m}) = \overline{W}_f$$

then the lifted equivalent of $\overline{W}_f$ is

$$W\overline{W}_fW^* \equiv \tilde{W}_f \tag{3.11}$$

Similarly,

$$W(S_{T/m}PH_{T/m})W^* = \tilde{P} \tag{3.12}$$

So, the modified problem is given by Fig. 3.9 where $\tilde{C}$ is the lifted equivalent of $\overline{C}$

$$\tilde{C} := W\overline{C}W^* \tag{3.13}$$

We have, thus, converted a time varying problem in lower dimensional I/O space into a time invariant problem in a higher dimensional I/O space. In order to compare the controller performance for various control sampling rates, i.e., m, all the design cases will be lifted to T/n, where n is a common multiple of various values of m, adopting Meyer's approach (1990).

The operator H which has been defined in (3.6) as

$$H := WS_{T/m}H_T\overline{S}_mW^*$$

can be rewritten as

$$H = \begin{bmatrix} 1 & 0 & .. & 0 \\ 1 & 0 & .. & 0 \\ 1 & 0 & .. & 0 \\ 1 & 0 & .. & 0 \end{bmatrix}_{m\times m} \tag{3.14}$$

The controller $\tilde{C}$ is nothing but the lifting of the controller $\overline{C}$ into a higher dimensional space. $\tilde{C}$ maps vector signal $\tilde{y}$ to vector signal $\tilde{u}$. The lifted controller $\tilde{C}$ must have a block toeplitz structure. A block toeplitz structure implies the controller is causal and time invariant, i.e., the convolution operator has a lower triangular structure with identical elements along each diagonal (including sub-diagonals). As a causal controller is required this constraint must be imposed (Khargonekar et al., 1985). This implies that the "D" matrix of $\tilde{C}$ is lower triangular. This ensures that the controller in the process of being lifted does not violate its causality constraints. This constraint must be strictly imposed when one solves for the controller and this is normally difficult. However, in our problem the operator H due to its special structure ensures that controller automatically satisfies this constraint. Thus, one can carry out the design without actually considering this constraint. This is verified below.

Let the operator H be combined with $\tilde{C}$. This is equivalent to

$$\tilde{u} = \begin{bmatrix} \overline{u}(mk) \\ \overline{u}(mk+1) \\ \\ \overline{u}(mk+m-1) \end{bmatrix} = \begin{bmatrix} \tilde{C}_{11} & \tilde{C}_{12} & \cdot & \cdot & \tilde{C}_{1m} \\ \tilde{C}_{21} & \cdot & \cdot & \cdot & \tilde{C}_{2m} \\ \vdots & \vdots & \vdots & \vdots & \vdots \\ \tilde{C}_{m1} & \tilde{C}_{m2} & \cdot & \cdot & \tilde{C}_{mm} \end{bmatrix} \cdot \times \begin{bmatrix} 1 & 0 & 0 & \cdot & 0 \\ 1 & 0 & 0 & \cdot & 0 \\ \vdots & \vdots & \vdots & \vdots & \vdots \\ 1 & 0 & 0 & \cdot & 0 \end{bmatrix} \begin{pmatrix} \overline{y}(mk) \\ \overline{y}(mk+1) \\ \vdots \\ \overline{y}(mk+m-1) \end{pmatrix} \tag{3.15}$$

$$\tilde{u} = \begin{bmatrix} C_{11} & 0 & 0 & \cdot & 0 \\ C_{21} & 0 & 0 & \cdot & 0 \\ \vdots & \vdots & \vdots & \vdots & \vdots \\ C_{m1} & 0 & \cdot & \cdot & 0 \end{bmatrix} \begin{pmatrix} \overline{y}(mk) \\ \overline{y}(mk+1) \\ \vdots \\ \overline{y}(mk+m-1) \end{pmatrix} = \begin{bmatrix} C_{11} \\ C_{21} \\ \vdots \\ C_{m1} \end{bmatrix} \overline{y}(mk) \tag{3.16}$$

where,

$$C_{i1} = \sum_{j=1}^{m} \tilde{C}_{ij}, \quad \text{for all } i, j = 1, 2, .., m \tag{3.17}$$

This implies that one needs to only solve for C_{i1}. The elements of $\tilde{C}$ can be arbitrarily chosen as long as they satisfy (3.17) and the causality constraint. This is an important observation because it indicates the inherent "two block" nature of the above problem, i.e., the measurement vector contains redundant information, and, when all redundancies are removed, the measurement vector reduces to a scalar. This is obvious from (3.16).

So far, we have viewed the controller obtained as a m-periodic controller. But, now we present an observation which is due to the special structure associated with this problem. Note that a linear shift invariant system (LSI) can be viewed as a m-periodic system, i.e., a LSI discrete time system with transfer matrix $\overline{C}(z)$ can be uniquely expressed as

$$\overline{C}(z) = \overline{C}_1(z^m) + z^{-1}\overline{C}_2(z^m) + ... + z^{-(m-1)}\overline{C}_m(z^m) \tag{3.18}$$

Thus, the lifting of $\overline{C}(z)$ produces

$$\tilde{C} = W\overline{C}W^{-1} = \begin{bmatrix} \overline{C}_1(z) & z^{-1}\overline{C}_m(z) & z^{-1}\overline{C}_{m-1}(z) & \cdot & z^{-1}\overline{C}_2(z) \\ \overline{C}_2(z) & \overline{C}_1(z) & z^{-1}\overline{C}_m(z) & \cdot & z^{-1}\overline{C}_3(z) \\ \vdots & \vdots & \vdots & \vdots & \vdots \\ \overline{C}_m(z) & \overline{C}_{m-1}(z) & \overline{C}_{m-2}(z) & \cdot & \overline{C}_1(z) \end{bmatrix} \tag{3.19}$$

i.e., a LSI discrete time system when viewed as a periodic system has only m independent elements unlike a m-periodic system which has m^2 independent elements. Recall that the lifted realization of the controller when combined with the operator H has a special structure, namely, it is a $m\times m$ block matrix with only its first column being nonzero. This implies that our controller can be thought to have only m independent elements.

Let us assume that the controller in its original domain is LSI. Then its lifting should correspond to the form as in (3.19). When (3.19) is combined with operator H we obtain a $m\times m$ block matrix with only its first column being nonzero, i.e.,

$$\tilde{C}(z)H = \begin{bmatrix} \overline{C}_1(z) + z^{-1}\overline{C}_m(z) + z^{-1}\overline{C}_{m-1}(z) + ... + z^{-1}\overline{C}_2(z) & 0 & \cdot & \cdot & 0 \\ \overline{C}_2(z) + \overline{C}_1(z) + z^{-1}\overline{C}_m(z) + ... + z^{-1}\overline{C}_3(z) & 0 & \cdot & \cdot & 0 \\ \vdots & \vdots & \vdots & \vdots & \vdots \\ \overline{C}_m(z) + \overline{C}_{m-1}(z) + \overline{C}_{m-2}(z) + ... + \overline{C}_1(z) & 0 & \cdot & \cdot & 0 \end{bmatrix} \tag{3.20}$$

Downloaded 08 Sep 2010 to 130.126.137.86. Redistribution subject to ASME license or copyright; see http://www.asme.org/terms/Terms_Use.cfm

Hence, from the definition of lifting we have

$$\tilde{C}(z)H=\begin{bmatrix} \overline{C}_1(z)+z^{-1}\overline{C}_m(z)+z^{-1}\overline{C}_{m-1}(z)+\ldots+z^{-1}\overline{C}_2(z) & 0 & \cdot & \cdot & 0 \\ \overline{C}_2(z)+\overline{C}_1(z)+z^{-1}\overline{C}_m(z)+\ldots+z^{-1}\overline{C}_3(z) & 0 & \cdot & \cdot & 0 \\ \vdots & \vdots & \vdots & \vdots & \vdots \\ \overline{C}_m(z)+\overline{C}_{m-1}(z)+\overline{C}_{m-2}(z)+\ldots+\overline{C}_1(z) & 0 & \cdot & \cdot & 0 \end{bmatrix}=\begin{bmatrix} C_{11} & 0 & 0 & \cdot & 0 \\ C_{21} & 0 & 0 & \cdot & 0 \\ \vdots & \vdots & \vdots & \vdots & \vdots \\ C_{m1} & 0 & \cdot & \cdot & 0 \end{bmatrix}, \quad (3.21)$$

where the right-hand side is obtained from solving the l-1 optimization problem of (3.16). Thus,

$$\begin{bmatrix} 1 & z^{-1} & z^{-1} & \cdot & z^{-1} \\ 1 & 1 & z^{-1} & \cdot & z^{-1} \\ \cdot & \cdot & \cdot & \cdot & \cdot \\ 1 & \cdot & \cdot & 1 & z^{-1} \\ 1 & 1 & \cdot & \cdot & 1 \end{bmatrix}\begin{bmatrix} \overline{C}_1(z) \\ \overline{C}_2(z) \\ \cdot \\ \cdot \\ \overline{C}_m(z) \end{bmatrix}=\begin{bmatrix} C_{11}(z) \\ C_{21}(z) \\ \cdot \\ \cdot \\ C_{m1}(z) \end{bmatrix} \quad (3.22)$$

The solution to the above system of equations is always non-trivial as the determinant is never equal to zero. The obtained solution when inserted into (3.18) yields a shift invariant controller in the original domain.

It must be noted here that the shift invariant realization of the controller is not specific for this problem alone but is true for the whole class of problems which give rise to the operator H, i.e., for all problems where the measurement is sampled at a slower rate than the generation of control signals and when the measurement rate is an integral multiple of control rate. Hence, for this class of problems the controller can be interpreted both as a periodic controller and a shift invariant controller. This means that the performance of shift invariant controllers in terms of robustness is as good as periodic controllers for this class of problems.

Before we conclude this section we state a theorem which shows the equivalence between the design in the original domain and the lifted domain.

Theorem 1: The controller $\overline{C}$ is the design controller for the original plant $\overline{G}$ iff the lifting of $\overline{C}$ given by $\tilde{C}$ is the design controller for the lifted problem $\tilde{G}$.

Proof: Let $\mathbf{F}(\overline{G}, \overline{C})$ denote the closed loop mapping of the original problem such that

$$\mathbf{F}(\overline{G}, \overline{C}): \overline{d}\rightarrow\overline{z}$$

The mapping for the lifted problem is given by

$\mathbf{F}(\tilde{G}, \tilde{C})$: $\tilde{d}\rightarrow\tilde{z}$

the two closed-loop mappings are related through the equation

$$\mathbf{F}(\tilde{G}, \tilde{C})=W\mathbf{F}(\overline{G}, \overline{C})W^{*} \quad (3.23)$$

but, mappings W and W^{*} are isometries

$$\Rightarrow \|\mathbf{F}(\tilde{G}, \tilde{C})\|=\|\mathbf{F}(\overline{G}, \overline{C})\| \quad (3.24)$$

Q.E.D

Here, $\overline{G}$ refers to the approximation of the generalized plant in Fig. 3.5 after the fictitious sample and hold are brought in and $\tilde{G}$ refers to the lifting of $\overline{G}$. Notice that as n in the fictitious sample and hold tends to infinity we get the original problem in Fig. 3.4.

This theorem states that the optimal controller for the lifted problem corresponding to Fig. 3.8, when lowered, is the optimal controller for the problem in Fig. 3.4 as n tends to infinity. The original problem is time varying while the lifted problem is time invariant. Hence it is simpler to carry out the design in the lifted domain and then lower the controller.

4 The l-1 Optimization Problem

In this section we formulate the l-1 optimization problem and state some facts about the l-1 norm (Vidyasagar, 1986; Dahleh et al., 1987; McDonald et al., 1991).

Definitions:

The space l^{∞} consists of bounded functions f: $Z^{+}\rightarrow R^{n}$

$$\text{s.t } \|f\|_{\infty}:=\sup_{k\in Z^{+}}\max_{1\le k\le n}|f(k)|<\infty \quad (4.1)$$

So, given $u, y\in l^{\infty}$ and a finite dimensional linear shift invariant system (FDLSI) $\overline{G}$

$$\text{s.t } y(k)=\overline{G}u(k)$$

then,

$$\|\overline{G}\|_{\infty-i}=\sup_{\|u\|_{\infty}}\frac{\|\overline{G}u\|_{\infty}}{\|u\|_{\infty}}=\|\overline{g}\|_{1} \quad (4.2)$$

where '$\overline{g}$' is the impulse response sequence of $\overline{G}$ whose elements are $m\times n$ matrices and

$$\|\overline{g}\|_{1}=\max_{1\le i\le m}\sum_{j=1}^{n}\sum_{k=0}^{\infty}|g_{ij}(k)| \quad (4.3)$$

Problem Formulation Given a FDLSI system $\overline{G}$ which has two vector inputs, namely, d the exogenous disturbance and u the control input, and two vector outputs, namely, z the regulated output and y the measurement, we wish to design a compensator K such that the closed loop system is internally stable and is optimal in the l-1 sense, i.e.,

$$\text{generalized plant: } \begin{pmatrix} z \\ y \end{pmatrix}=\begin{bmatrix} \overline{G}_{11} & \overline{G}_{12} \\ \overline{G}_{21} & \overline{G}_{22} \end{bmatrix}\begin{pmatrix} d \\ u \end{pmatrix},$$

$$\text{controller: } u=Ky.$$

The closed-loop transfer function from d to z is

$$\phi=\overline{G}_{11}+\overline{G}_{12}K(I-\overline{G}_{22}K)^{-1}\overline{G}_{21}. \quad (4.4)$$

Using YJBK parameterization the above equation can be rewritten as

$$\phi=\overline{H}-\overline{U}Q\overline{V} \quad (4.5)$$

where

$$\begin{aligned} \overline{H}&:=\overline{G}_{11}+\overline{G}_{12}M_R Y_L\overline{G}_{21} \\ \overline{U}&:=\overline{G}_{12}M_R \\ \overline{V}&:=M_L\overline{G}_{21} \end{aligned} \quad (4.6)$$

Q belongs to S where S is the ring of stabilizing functions in l-1, $\overline{G}_{22}=N_R M_R^{-1}=M_L^{-1}N_L$ are the left and right coprime factorizations.

Also, the following Bezout identity must be satisfied

$$\begin{bmatrix} X_L & -Y_L \\ -N_L & -M_L \end{bmatrix}\begin{bmatrix} M_R & Y_R \\ N_R & X_R \end{bmatrix}=I \quad (4.7)$$

The resulting compensator 'K' is given by

$$K=(Y_R-M_RQ)(X_R-N_RQ)^{-1}=(X_L-QN_L)^{-1}(Y_L-QM_L) \quad (4.8)$$

Hence, the optimization problem reduces to

$$\mu^{0}=\inf_{Q\in S}\|\overline{H}-\overline{U}Q\overline{V}\|_{1} \quad (4.9)$$

By the duality theorem, this problem can be posed in the dual space as

$$\mu^{0}=\inf_{Q\in S}\|\overline{H}-\overline{U}Q\overline{V}\|_{1}=\max_{\substack{G\in S^{\perp} \\ \|G\|_{\infty}\le 1}}\langle\overline{H}, G\rangle$$

Downloaded 08 Sep 2010 to 130.126.137.86. Redistribution subject to ASME license or copyright; see http://www.asme.org/terms/Terms_Use.cfm

Based on the number of inputs, regulated outputs, disturbances and measurements, a MIMO problem is classified as a "one block," "two block," or a "four block" problem. Since we have as many control inputs as the regulated outputs, but have fewer measurements than the disturbances, the multirate sampling problem, in the lifted domain poses itself as a "two block" problem, i.e., U is square ($n_w = n_u$) but V is fat ($n_y < n_z$). A recently proposed method called "Delay Augmentation technique" (Diaz-Bobillo, 1992) will be used to solve for the suboptimal solution.

where

$$A_{pd} = e^{A_p T/m} \quad \text{and} \quad B_{pd} = \left(\int_0^{T/m} e^{A_p t} dt \right) B_p.$$

Let x_w denote the state of $\tilde{W}_f$ and x_p denote the state of $\tilde{P}$ and define the augmented state vector

$$\xi := \begin{bmatrix} x_w \\ x_p \end{bmatrix}$$

Then the augmented plant is given by

$$\tilde{G} = \begin{bmatrix} \begin{bmatrix} A_{fd}^m & 0 \\ 0 & A_{pd}^m \end{bmatrix} & \begin{bmatrix} A_{fd}^{m-1} B_{fd} & \cdots & A_{fd} B_{fd} & B_{fd} \\ 0 & \cdots & 0 & 0 \end{bmatrix} & \begin{bmatrix} 0 & 0 & \cdots & 0 \\ A_{pd}^{m-1} B_{pd} & \cdots & A_{pd} B_{pd} & B_{pd} \end{bmatrix} \\ \begin{bmatrix} C_{fd} & C_{pd} \\ C_{fd} A_{fd} & C_{pd} A_{pd} \\ \cdot & \cdot \\ \cdot & \cdot \\ C_{fd} A_{fd}^{m-1} & C_{pd} A_{pd}^{m-1} \end{bmatrix} & \begin{bmatrix} D_f & 0 & \cdot & \cdot & 0 \\ C_{fd} B_{fd} & D_f & \cdot & \cdot & \cdot \\ \cdot & \cdot & \cdot & \cdot & \cdot \\ \cdot & \cdot & \cdot & \cdot & 0 \\ C_{fd} A_{fd}^{m-2} B_{fd} & \cdot & \cdot & C_{fd} B_{fd} & D_f \end{bmatrix} & \begin{bmatrix} D_p & 0 & 0 & \cdot & 0 \\ C_p B_{pd} & D_p & \cdot & \cdot & \cdot \\ \cdot & \cdot & \cdot & \cdot & \cdot \\ \cdot & \cdot & \cdot & \cdot & 0 \\ C_p A_{pd}^{m-2} B_{pd} & \cdot & \cdot & C_p B_{pd} & D_p \end{bmatrix} \\ [C_{fd} \quad C_{pd}] & [D_f \; 0 \; 0 \; . \quad 0] & [D_p \; 0 \; . \; . \quad 0] \end{bmatrix} \tag{5.4}$$

5 State Space Realizations in Lifted Domain

In this section we present the state space realizations of the lifted equivalents of the plant and the filter and form an augmented realizations for the case $n = m$.

$$\text{Let } W_f = \begin{bmatrix} A_f & B_f \\ C_f & D_f \end{bmatrix}$$

The discrete equivalent of W_f when sampled at T/m s is given by

$$\overline{W}_f = \begin{bmatrix} A_{fd} & B_{fd} \\ C_f & D_f \end{bmatrix}$$

where

$$A_{fd} = e^{A_f T/m}; \quad B_{fd} = \left(\int_0^{T/m} e^{A_f t} dt \right) B_f \tag{5.1}$$

Then the lifted system $\tilde{W}_f$ is given by

$$\tilde{W}_f = \begin{bmatrix} A_{fd}^m & [A_{fd}^{m-1} B_{fd} & \cdots & A_{fd} B_{fd} & B_{fd}] \\ \begin{bmatrix} C_f \\ C_f A_{fd} \\ \cdot \\ \cdot \\ C_f A_{fd}^{m-1} \end{bmatrix} & \begin{bmatrix} D_f & 0 & \cdot & \cdot & 0 \\ C_f B_{fd} & D_f & 0 & \cdot & 0 \\ C_f A_{fd} B_{fd} & C_f B_{fd} & \cdot & & \\ \cdot & \cdot & \cdot & \cdot & \\ C_f A_{fd}^{m-2} B_{fd} & \cdot & C_f A_{fd} B_{fd} & C_f B_{fd} & D_f \end{bmatrix} \end{bmatrix} \tag{5.2}$$

$$\text{Let } P = \begin{bmatrix} A_p & B_p \\ C_p & D_p \end{bmatrix}$$

The lifted plant is

$$\tilde{P} = \begin{bmatrix} A_{pd}^m & [A_{pd}^{m-1} B_{pd} & \cdots & A_{pd} B_{pd} & B_{pd}] \\ \begin{bmatrix} C_p \\ C_p A_{pd} \\ \cdot \\ \cdot \\ C_p A_{pd}^{m-1} \end{bmatrix} & \begin{bmatrix} D_p & 0 & \cdot & \cdot & 0 \\ C_p B_{pd} & D_p & \cdot & \cdot & \cdot \\ \cdot & C_p B_{pd} & \cdot & & \cdot \\ \cdot & \cdot & \cdot & \cdot & 0 \\ C_p A_{pd}^{m-2} B_{pd} & \cdot & \cdot & C_p B_{pd} & D_p \end{bmatrix} \end{bmatrix} \tag{5.3}$$

Note that the 'C' matrix corresponding to measurement has a rank equal to that of the original problem. This is because the operator 'H' has been absorbed into the controller.

Assuming that the sampling rates are nonpathological and that (A_f, B_f) and (A_p, B_p) are stabilizable and (C_f, A_f) and (C_p, A_p) are detectable we can state the following theorem.

If the sampling rate is nonpathological then the lifted system is detectable and stabilizable if and only if the original system is detectable and stabilizable (Khargonekar, 1985). Hence the augmented plant $\tilde{G}$ is stabilizable through $\tilde{u}(k)$. If the hold operator were not present, $\bar{y}(k)$ and $\tilde{z}(k)$ are identical. Therefore, we can conclude that $\tilde{G}$ is detectable through $\tilde{z}$. In the presence of the operator H, for the system to be detectable through $\bar{y}(k)$, the rank of the following matrix must be equal to 'n' for all $\text{Re}(\lambda) > 0$:

$$\rho \left[\begin{bmatrix} A_{fd} & 0 \\ 0 & A_{pd} \end{bmatrix} \right] = n \tag{5.5}$$

Assuming that the sampling times T and T/m are nonpathelogical the rank of the above matrix is always equal to 'n'. Hence the augmented plant $\tilde{G}$ is stabilizable and detectable (also refer to Theorem 3 in Rahmani et al., 1990).

6 Numerical Examples

In this section we present the procedure for the design of a multirate controller. We also present some simulation results for the multirate controller and compare it with a PD controller.

Consider a DC servo motor driven linear ball screw actuator. The open-loop transfer function of the plant has been obtained from a signal analyzer:

$$P(s) = \frac{-0.0632(s + 4749.3)(s + 1934.7)}{s[(s + 953.72)^2 + (841.02)^2]} \tag{6.1}$$

The delay in the vision system was approximately equal to 100 ms (this includes the image acquisition and image processing time). The gain of the vision system was assumed to be I, i.e., we assumed that the camera completely recovers the spatial configuration of the object from visual information.

As we are interested only in tracking signals of low fre-

Downloaded 08 Sep 2010 to 130.126.137.86. Redistribution subject to ASME license or copyright; see http://www.asme.org/terms/Terms_Use.cfm

quency, we approximate the delay in vision by a pade' approximation:

$$e^{-Ts} \cong \frac{(1-Ts)}{(1+Ts)} \tag{6.2}$$

Hence, the t plant model is given by

$$P(s) = \frac{0.0632(s-10)(s+4749.3)(s+1934.7)}{s(s+10)[(s+953.72)^2+(841.02)^2]} \tag{6.3}$$

In order to eliminate the high frequency components of the reference signal, a strictly proper first order filter was used

$$W_f = \frac{1}{(s+1)} \tag{6.4}$$

Notice that the plant has a pole at $s=0$. In the l-1 design a pole on the unit circle leads to a controller of a very high order. In order to avoid a very high order controller we chose to perturb the pole at $s=0$ into the left half plane. So, the design plant transfer function is

$$P(s) = \frac{0.0632(s-10)(s+4749.3)(s+1934.7)}{(s+0.01)(s+10)[(s+953.72)^2+(841.02)^2]} \tag{6.5}$$

The design of the multirate controller was carried out for various sampling rates of the controller (which are of the form T/n where n is an integer and T is the vision sampling time). For each sampling rate an optimal l-1 controller was found and the closed-loop l-1 norm evaluated. The evaluation was stopped at $T/6$ as no substantial norm improvements were obtained. The design procedure is elucidated for $T/6$ sampling rate. The lifting of the original plant using (4.4) for $T/6$ sampling rate gives

$$\tilde{G} = \begin{bmatrix} A_g & B_{1g} & B_{2g} \\ C_{1g} & D_{11g} & D_{12g} \\ C_{2g} & D_{21g} & D_{22g} \end{bmatrix}$$

$$D_{11g} = \begin{bmatrix} 0 & 0 & 0 & 0 & 0 & 0 \\ 0.0165 & 0 & 0 & 0 & 0 & 0 \\ 0.0163 & 0.0165 & 0 & 0 & 0 & 0 \\ 0.0160 & 0.0163 & 0.0165 & 0 & 0 & 0 \\ 0.0157 & 0.0160 & 0.0163 & 0.0165 & 0 & 0 \\ 0.0155 & 0.0157 & 0.0160 & 0.0163 & 0.0165 & 0 \end{bmatrix}$$

$$D_{12g} = \begin{bmatrix} 0 & 0 & 0 & 0 & 0 & 0 \\ -0.0050 & 0 & 0 & 0 & 0 & 0 \\ -0.0034 & -0.0050 & 0 & 0 & 0 & 0 \\ -0.0020 & -0.0034 & -0.0050 & 0 & 0 & 0 \\ -0.000 & -0.0020 & -0.0034 & -0.0050 & 0 & 0 \\ 0.0003 & -0.0007 & -0.0020 & -0.0034 & -0.0050 & 0 \end{bmatrix}$$

$$D_{21g} = [0\ 0\ 0\ 0\ 0\ 0]$$

$$D_{22g} = [0\ 0\ 0\ 0\ 0\ 0] \tag{6.6}$$

To perform the l-1 minimization we first obtain the Youla parameterization of $\tilde{G}$ into $\tilde{H}$ $\tilde{U}$ and $\tilde{V}$. Note that $\tilde{U}$ is square and $\tilde{V}$ is fat, i.e., we have as many control inputs as regulated outputs but have fewer measurements than the disturbance inputs. Thus the resulting problem is a 2-block problem. For a sampling rate of $T/6$ the optimal controller obtained has the following state space realization:

$$A_g = \begin{bmatrix} 9.0484e-01 & 0 & 0 & 0 & 0 \\ 0 & 2.3045e-05 & 4.3958e-02 & 3.7262e+01 & 3.7262e-01 \\ 0 & -2.3045e-06 & -4.3958e-03 & -3.7262e+00 & -3.7162e-02 \\ 0 & 2.2984e-07 & 4.3839e-04 & 3.7161e-01 & -6.2739e-03 \\ 0 & 3.8802e-08 & 7.4631e-05 & 6.3918e-02 & 9.9964e-01 \end{bmatrix}$$

$$B_{2g} = \begin{bmatrix} 0 & 0 & 0 & 0 & 0 & 0 \\ 4.18e-7 & 4.94e-7 & 5.83e-7 & 6.89e-7 & 8.14e-7 & -5.30e-6 \\ -4.18e-8 & -4.94e-8 & -5.83e-8 & -6.89e-8 & -8.14e-8 & 5.3e-7 \\ 4.17e-9 & 4.92e-9 & 5.82e-9 & 6.88e-9 & 8.13e-9 & 8.87e-9 \\ 6.13e-10 & 5.37e-10 & 4.48e-10 & 3.42e-10 & 2.16e-10 & 7.05e-11 \end{bmatrix}$$

$$B_{1g} = \begin{bmatrix} 0.0152 & 0.0155 & 0.0157 & 0.0160 & 0.0163 & 0.0165 \\ 0 & 0 & 0 & 0 & 0 & 0 \\ 0 & 0 & 0 & 0 & 0 & 0 \\ 0 & 0 & 0 & 0 & 0 & 0 \\ 0 & 0 & 0 & 0 & 0 & 0 \end{bmatrix}$$

$$C_{1g} = \begin{bmatrix} 1.0 & -6.34e-2 & -4.26e+2 & -5.84e+5 & 5.88e+6 \\ 9.84e-1 & -2.55e-1 & -4.82e+2 & -4.05e+5 & 5.88e+6 \\ 9.67e-1 & -1.5976e-1 & -3.01e+2 & -2.51e+5 & 5.88e+6 \\ 9.51e-1 & -7.94e-2 & -1.48e+2 & -1.214e+5 & 5.88e+6 \\ 9.36e-1 & -1.13e-2 & -1.8e+1 & 1.14e+4 & 5.88e+6 \\ 9.24e-1 & 4.62e-2 & 9.18e+1 & 8.17e+4 & 5.88e+6 \end{bmatrix}$$

$$C_{2g} = [1.0\ \ -6.34e-2\ \ -4.26e+2\ \ -5.84e+5\ \ 5.88e+6]$$

Downloaded 08 Sep 2010 to 130.126.137.86. Redistribution subject to ASME license or copyright; see http://www.asme.org/terms/Terms_Use.cfm

Table 6.1 Comparison of l-1 optimal control and PD control

Delay in the vision unit (s)	Sampling rate of controller (s)	l-1 norm at sampling rate of the controller	l-1 norm at T/6 (=0.0167) sampling rate	l-1 norm of PD at sampling rate of the controller
0.1	0.1 (n=1)	0.21278	0.21300	0.4994
0.1	0.05 (n=2)	0.19657	0.19721	0.5045
0.1	0.033 (n=3)	0.19053	0.19134	0.5126
0.1	0.025 (n=4)	0.18739	—	0.5160
0.1	0.02 (n=5)	0.18546	—	0.5186
0.1	0.0167 (n=6)	0.18415	0.18415	0.5202
0.0167	0.0167	0.11325	0.11325	NA

$$\tilde{C}=\begin{bmatrix} A_c & B_c \\ C_c & D_c \end{bmatrix}$$

$$A_c=\begin{bmatrix} -0.93542 & -0.15127 & -0.23215 \\ 1.4756e-2 & 0.90363 & -7.8839e-2 \\ 2.4772e-7 & 3.1957e-5 & -1.1244e-6 \end{bmatrix}$$

$$B_c=\begin{bmatrix} 3.5772e1 \\ 8.1731 \\ 1.3721e-4 \end{bmatrix}$$

$$C_c=\begin{bmatrix} 8.7490 & -0.60214 & 0.41432 \\ -0.30768 & 0.14036 & 9.9729e-2 \\ 0.67358 & 5.7798e-2 & 0.13179 \\ 0.55553 & 6.5630e-2 & 1.2592e-1 \\ 0.5807 & 6.3582e-2 & 0.12425 \\ 0.54757 & 6.2636e-02 & 0.12215 \end{bmatrix}$$

$$D_c=\begin{bmatrix} -1.6896e2 \\ -4.6420 \\ -2.2258e1 \\ -1.9952e1 \\ -1.9835e1 \\ -1.9485e1 \end{bmatrix} \tag{6.7}$$

Note that the above realization corresponds to the lifting of $\bar{C}$. When $\tilde{C}$ is lowered, we obtain a 6-periodic controller:

$$\bar{C}=[C_{11}\ C_{21}\ C_{31}\ C_{41}\ C_{51}\ C_{61}]' \tag{6.8}$$

where C_i for $i=[1, 2, 3, .. 6]$ are time invariant controllers which form the 6-periodic controller.

where,

$$C_{11}(z)=\frac{-168.9(z-2.93e-8)[(z-0.896)^2+(0.349)^2]}{(z+9.342e-1)(z-9.024e-1)(z-1.7358e-06)} \tag{6.9}$$

$$C_{21}(z)=\frac{-4.642(z-1.05e-8)(z-1.038)(z+3.194)}{(z+9.342e-1)(z-9.024e-1)(z-1.7358e-06)} \tag{6.10}$$

$$C_{31}(z)=\frac{-22.26(z-1.046e-7)(z-0.9046)(z-0.1673)}{(z+9.342e-1)(z-9.024e-1)(z-1.7358e-06)} \tag{6.11}$$

$$C_{41}(z)=\frac{-19.95(z-2.261e-7)(z-0.9211)(z-7.00e-2)}{(z+9.342e-1)(z-9.024e-1)(z-1.7358e-06)} \tag{6.12}$$

$$C_{51}(z)=\frac{-19.84(z-3.536e-7)(z-0.9183)(z-0.1234)}{(z+9.342e-1)(z-9.024e-1)(z-1.7358e-06)} \tag{6.13}$$

$$C_{61}(z)=\frac{-19.46(z-1.986e-7)(z-0.9195)(z-8.03e-2)}{(z+9.342e-1)(z-9.024e-1)(z-1.7358e-06)} \tag{6.14}$$

Each of the above controllers has a sampling time of 0.1 s. The convolution of $\bar{C}$ is a combination of the convolutions of C_i for $i=[1, 2, 3, .., 6]$.

The equivalent shift invariant realization of the controller aforementioned can be obtained by solving (3.22) and (3.18). Thus, the LSI realization $\bar{C}(z)$ is given by

$$\bar{C}(z)=\frac{N(z)}{D(z)}$$

$$N(z)=[-168.9z^{24}+164.26z^{23}-17.62z^{22}+2.31z^{21}+0.11z^{20}+0.38z^{19}+322.13z^{18}-312.68z^{17}+33.87z^{16}-4.09z^{15}+0.895z^{14}-1.21z^{13}-175.62z^{12}+171.56z^{11}-18.76z^{10}+2.08z^{9}-0.962z^{8}+0.811z^{7}+1.44z^{6}-4.73\times10^{-6}z^{5}+5.14\times10^{-7}z^{4}-6.15\times10^{-8}z^{3}+5.04\times10^{-7}z^{2}-5.10\times10^{-7}z-2.85\times10^{-7}]$$

$$D(z)=(z^6-1)(z^{18}+3.18\times10^{-2}z^{12}-0.843z^{6}+1.463\times10^{-6}) \tag{6.16}$$

The optimal $l-1$ norms for various sampling rates of the controller, assuming that the delay in vision unit is 0.1 s, is shown in Table 6.1. Also, a PD controller of the form

$$\bar{C}=K_p+\frac{K_D(1-z^{-1})}{T_s} \tag{6.17}$$

where, K_p is the proportional gain, K_D the derivative gain, and T_s is the sampling rate of the PD controller, was designed and its l-1 norm was evaluated using the lifting technique and compared with the optimal multirate controller. The PD controller was tuned to minimize the spectral radius of the single rate discrete time system for 0.1 second sampling time, resulting in $K_P=-6$ and $K_D=-1.25$.

The first column of Table 6.1 represents the delay time in the vision unit. The second column represents the sampling rate of the controller which for our design also gives the sampling rate of the fictitious sample and hold. Column three gives the l-1 norm of the closed loop system optimal at the sampling rate of the controller. Column four gives the l-1 norms of the closed loop systems calculated at $T/6$ sampling rate. The significance of this column is twofold: First, it provides us a means to compare the performance of designs which use controllers operating at different sampling rates; Second, we evaluate the control system performance for Fig. 3.1, i.e., the sampled data system, by the use of Fig. 3.8, i.e., discrete approximation of Fig. 3.1 (the calculation uses $n=6$ although n could be larger for better approximation). In order to lift the cases for T/4 and T/5, the system must be lifted to dimension corresponding to a sampling rate of T/60, which requires intensive computation and is omitted. As expected, the performance improves with decreasing controller sampling time. If a fast vision unit operating at T/6 was possible, the performance would be as given in the last row. The performance of the multirate controllers, i.e., row two through row

Downloaded 08 Sep 2010 to 130.126.137.86. Redistribution subject to ASME license or copyright; see http://www.asme.org/terms/Terms_Use.cfm

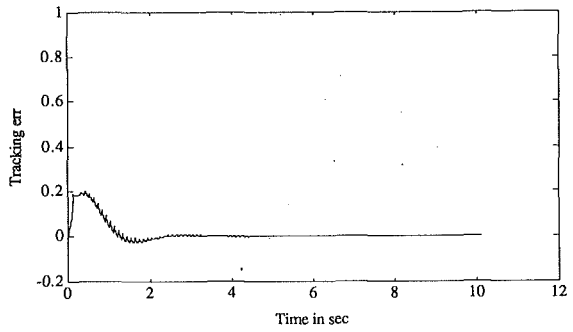

Fig. 6.1 Response of the closed-loop system to a filtered step input

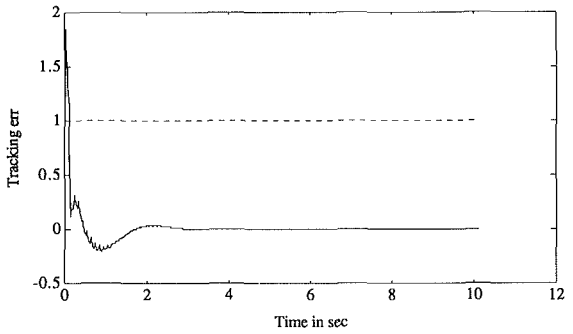

Fig. 6.2 Response of the closed-loop system to an unfiltered step input

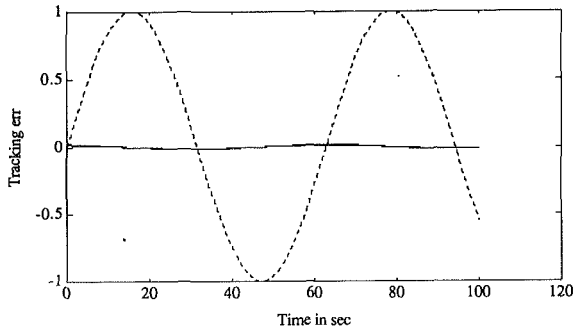

Fig. 6.3 Response of the closed-loop system to an unfiltered sine wave, $\omega = 0.1$ rad/s

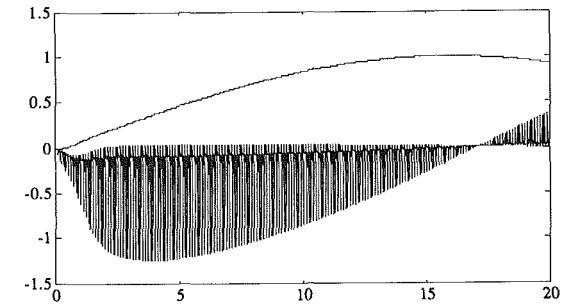

Fig. 6.4 Output of the multirate controller. The chattering curve is the controller output and the smooth curve is the camera output.

six, are between the fast and the slow single rate controllers as in row seven and row one, respectively. Thus, multirate control can be thought of as an alternative to single rate control when a fast sensor is not available. We can see from Table 6.1 that the l-1 designs have a much smaller l-1 norm than the PD design. This proves the superiority of *a* the optimal l-1 multirate controller design over conventional design techniques.

The performance of the 6-periodic controller in feedback with the X-Y table was simulated for various exogeneous signals. The simulation was carried out in the lifted domain as the closed loop system in this domain is shift invariant. The performance of the closed-loop system was simulated with and without the filter, with the filter to verify the l-1 design and without the filter to simulate the realistic performance. The simulation results are given below.

Figure 6.1 shows the response of the closed-loop system when the disturbances enter the system through the filter. Notice that the maximum tracking error corresponds to the one obtained from the design. Figure 6.2 shows the response of the actual system to a step disturbance. Notice that the oscillations in the output are minimal. This is a typical feature of l-1 designs. The response of the closed-loop system to a sine wave disturbance with $\omega = 0.1$ rad/s is shown in Fig. 6.3. The response with and without the filter are nearly the same as to be expected. These simulations confirm the good performance obtainable from the l-1 multirate controller. The controller output of the simulation in Fig. 6.3 is shown in Fig. 6.4, the chattering behavior indicating the 6-modes of the multirate controller.

7 Conclusions

The analysis and design of a multirate visual feedback servo control system have been studied. We have shown that the lifting technique provides a useful tool for analyzing and designing multirate control systems and have further derived some intrinsic properties useful for control system design and implementation. These results hold for the class of slow sensing and fast control multirate problems in general. The l-1 norm minimization provides a direct means to meet both the camera field of view limit and mechanical motion tolerance constraints. The numerical example demonstrates the methodology and provides performance comparisons among different sampling rates and control algorithms.

Acknowledgment

The authors wish to thank Professor Bamieh for some useful discussions and Professor Diaz-Bobillo and Professor Dahleh of Massachusetts Institute of Technology for providing the l-1 optimization software used in this work. This work was supported in part by National Science Foundation under grant no. DDM-9114001 and by State of Illinois through University of Illinois Manufacturing Research Center Multi-Chip Module Packaging Program.

References

Allen, P., Yoshimi, B., and Timcenko, A., 1991, "Real Time Visual Servoing," IEEE Int'l. Conference on Robotics and Automation, pp. 851–856.

Al-Rahmani, H. M., and Franklin, G. F., 1990, "A New Optimal Multirate Control of Linear Periodic and Time Invariant Systems," *IEEE Trans. Automatic Control*, Vol. AC-35, pp. 406–415.

Bamieh, B. A., and Pearson, J. B., 1992, "A General Framework for Linear Periodic Systems with Applications to H^{∞} Sapled-Data Control," *IEEE Trans. Automatic Control*, Vol. AC-37, pp. 418–435.

Dahleh, M. A., and Pearson, J. B., 1987, "l-1-Optimal Feedback Controllers for MIMO Discrete Time Systems," *IEEE Trans. Automatic Control*, Vol. AC-32, pp. 314–322.

Dahleh, M. A., Voulgaris, P. G., and Valavani, L. S., 1992, "Optimal and Robust Controllers for Periodic and Multirate Systems," *IEEE Trans. Automatic Control*, Vol. AC-37, pp. 90–99.

Diaz-Bobillo, I. J., 1992, "The General l-1 Optimal Multiblock Problem: Exact and Approximate Solutions," Ph.D. thesis Report No. LIDS-TH-2093, Massachusetts Institute of Technology, Feb.

Dullerud, G. E., and Francis, B. A., 1992, "L-1 Analysis and Design of Sampled-Data Systems," *IEEE Trans. Automatic Control*, Vol. AC-37, pp. 436–446.

Francis, B. A., and Georgiou, T. T., 1988, "Stability Theory for Linear Time Invariant Plants with Periodic Digital Controllers," *IEEE Trans. Automatic Control*, Vol. AC-33, pp. 820–832.

Feddema, J. T., and Mitchell, O. R., 1989, "Vision-Guided Servoing with

Downloaded 08 Sep 2010 to 130.126.137.86. Redistribution subject to ASME license or copyright; see http://www.asme.org/terms/Terms_Use.cfm

Feature Based Trajectory Generation," *IEEE Trans. on Robotics and Automation*, pp. 691-700.

Khargonekar, P. P., Poolla, K., and Tannenbaum, A., 1985, "Robust Control of Linear Time Invariant Plants Using Periodic Compensation," *IEEE Trans. Automatic Control*, Vol. AC-30, pp. 1088-1096.

McDonald, J. S., and Pearson, J. B., 1991, "*l*-1 Optimal Control of Multivariable Systems with Output Norm Constraints," *Automtica*, Vol. 27, pp. 317-329.

Meyer, D. G., 1990, "A New Class of Shift Varying Operators, Their Shift Invariant Equivalents, and Multirate Digital Systems," *IEEE Trans. Automatic Control*, Vol. AC-35, pp. 429-433.

Meyer, R. A., and Burrus, C. S., 1975, "A Unified Analysis of Multirate and Periodically Time Varying Digital Filters," *IEEE Trans. Circuits and Systems*, Vol. CAS-22, pp. 162-168.

Papanikolopoulos, N., Khosla, P. K., and Kanade, T., 1991, "Adaptive Robotic Visual Tracking," IEEE Int'l. Conference on Robotics and Automation, pp. 857-864.

Skaar, S. B., Brockman, W. H., and Hanson, R., 1987, "Camera-Space Manipulation," *International Journal for Robotics Research*, pp. 20-32.

Vidyasagar, M., 1986, "Optimal Rejection of Persistent Bounded Disturbances," *IEEE Trans. Automatic Control*, Vol. AC-31.

Weiss, L. E., Sanderson, A. C., and Neuman, C. P., 1987, "Dynamic Sensor Based Control of Robots with Visual Feedback," *IEEE Trans. on Robotics and Automation*, pp. 404-417.

Downloaded 08 Sep 2010 to 130.126.137.86. Redistribution subject to ASME license or copyright; see http://www.asme.org/terms/Terms_Use.cfm